OPEN

NPG Asia Materials (2016) 8, e322; doi:10.1038/am.2016.158
www.nature.com/am

ORIGINAL ARTICLE

Giant electrorheological fluids with ultrahigh electrorheological efficiency based on a micro/nano hybrid calcium titanyl oxalate composite

Jinghua Wu[1], Zhenyang Song[1], Fenghua Liu[1], Jianjun Guo[1], Yuchuan Cheng[1,2], Shengqian Ma[2] and Gaojie Xu[1]

A novel micro/nanoparticle hybrid calcium titanyl oxalate electrorheological (ER) material composed of micron-sized spindly particles and nanometer-sized irregular particles was successfully fabricated. The giant ER fluid based on the composite exhibits enhanced not only yield stress but also low field-off viscosity, thereby resulting in an ultrahigh ER efficiency that greatly exceeds that of any existing giant ER (GER) material. The synergistic effect between the spindly microparticles and irregular nanoparticles discovered in this study suggests a promising method for solving the long-standing ER efficiency problems. Moreover, the one-step synthesis approach presented in this work can be readily expanded for mass production of other GER materials in practical applications.
NPG Asia Materials (2016) **8,** e322; doi:10.1038/am.2016.158; published online 4 November 2016

INTRODUCTION

Electrorheological (ER) fluids, which exhibit flow behavior and rheological properties that can be tuned in a controlled manner using an external electric field, are some of the most attractive smart materials.[1,2] ER fluid is generally a suspension consisting of polarizable particles dispersed in a nonpolar liquid medium. Applying an external electric field changes ER fluid from a liquid to a nearly solid state within milliseconds, with an accompanying orders of magnitude increase in yield stress and shear modulus; furthermore, this effect completely and rapidly reverses once the field is removed.[3–8] These features have made ER fluids the focus of numerous scientific investigations because of their potential application for actively controlling various devices with electric–mechanical interfaces.[9,10] Coupled with sensors to trigger the external electric field, ER fluids can turn many devices, such as clutches, valves and dampers, into active mechanical elements that are capable of responding to environmental variations. Despite these advantages, ER fluids have suffered as a result of their inferior yield stress, which yields poor mechanical performance that limits their application.[11–14] The discovery of the giant ER (GER) effect has revived interest in this area. Compared with conventional ER fluids, GER fluids exhibit yield stresses that are almost an order of magnitude higher. The polarization of molecular dipoles in the contact region between two neighboring nanoparticles is thought to be responsible for the GER effect.[15–17] Various inorganic and organic/inorganic GER materials have been synthesized;[18–27] for example, Wen *et al.*[18] reported a new type of GER fluid consisting of polar group-modified nano-sized barium titanyl oxalate particles suspended in silicone oil.

Recently, the development of high-performance ER materials has been promoted to meet the rapid growth in the demand for practical applications. ER efficiency reflects an achievable increase in the mechanical strength during application of an electric field. A material with high ER efficiency exhibits high-yield stress under an electric field and low field-off viscosity. According to GER theory, yield stress displays an opposite dependence on particle size.[28] Therefore, most giant ER materials reported to date are composed of nanometer-sized particles. However, the particle size effect is a trade-off effect, because nanometer-sized particles are always accompanied by a high viscosity in the absence of an electric field, which would lead to low ER efficiency.[24–27] Therefore, it remains a challenge to obtain ER materials with high efficiency.

Particle morphology is considered a critical factor influencing ER fluid performance.[29] Recent theoretical and experimental works have shown that anisotropic particles can induce large polarizability within short relaxation times, which can further enhance the yield stress.[30,31] In our previous study, we fabricated a series of one-dimensional ER TiO_x-based nanoparticles. By observing the structure under an applied electric field, the overlap of one-dimensional particles effectively prevents the chain structure from breaking down, which provides enhanced-yield stress and structural stability. Consequently, the ER

[1]Zhejiang Key Laboratory of Additive Manufacturing Materials, Ningbo Institute of Materials Technology and Engineering, Chinese Academy of Sciences, Ningbo, China and [2]Department of Chemistry, University of South Florida, Tampa, FL, USA
Correspondence: Dr Y Cheng, Zhejiang Key Laboratory of Additive Manufacturing Materials, Ningbo Institute of Materials Technology and Engineering, Chinese Academy of Sciences, 1219 Zhongguan West Road, Ningbo, Zhejiang 315201, China.
E-mail: yccheng@nimte.ac.cn
or Professor S Ma, Department of Chemistry, University of South Florida, CHE 205A, 4202 East Fowler Avenue, Tampa, FL 33620, USA.
E-mail: sqma@usf.edu
Received 17 May 2016; revised 26 July 2016; accepted 9 August 2016

efficiency of the ER fluid based on nanorods is higher than that of the ER fluid based on nanospheres. However, the suspensions of the anisotropic nanoparticles still possess high field-off viscosities due to the relatively small sizes of the nanoparticles. To achieve both high-yield stress and low field-off viscosity, an effective strategy can involve the mixing of large particles with small particles. In the presence of an electric field, the large anisotropic one-dimensional particles are oriented along the electric field direction and form a chain structure, and the small particles gather at the contact area between two neighboring anisotropic particles; such a unique structure is therefore expected to enhance the yield stress. When no electric field is applied, a shear flow rotates the large anisotropic particles along the direction of the shear force, thus dramatically decreasing the fluid viscosity.

Calcium titanyl oxalate (CTO) is one of the most promising GER materials among the discovered ER materials due to its high ER activity, low leakage current and ease of preparation. In this report, we report a facile one-step method to synthesize a micro/nanoparticle hybrid CTO (HCTO) composite, which contains anisotropic spindly microparticles and irregular nanoparticles. The GER fluid based on the composite exhibits not only enhanced-yield stress but also low field-off viscosity, thereby resulting in an ultrahigh ER efficiency that far exceeds that of previously reported GER materials. The synergistic effect between the spindly microparticles and irregular nanoparticles as discovered from our studies thus suggests a promising way for solving the long-standing ER efficiency problems. Moreover, the one-step synthesis approach presented in this work can be readily expanded for mass production of other GER materials in practical applications.

MATERIALS AND METHODS

Materials

Tetrabutyl titanate (98%), anhydrous calcium chloride ($CaCl_2$, A.R.) and oxalic acid ($H_2C_2O_4{\cdot}2H_2O$, A.R.) were purchased from the Sinopharm Chemical Reagent Company (Shanghai, China). Silicone oils ($\eta = 50$ mPa s^{-1}, 25 °C) were obtained from Hangping Company (Beijing, China). The viscosity of the methyl-terminated silicone oils depends on the degree of polymerization and hence the length of the polymer chain. All of these chemicals were used as received without further purification. Deionized water from a Millipore-Q purification system (Millipore, Billerica, MA, USA) with a resistivity of 18.2 MΩ cm was used in this work.

Preparation of micro/nanoparticle HCTO composites

The HCTO composites were synthesized via a precipitation process. First, 11.6 ml of titanium butoxide was dissolved in 100 ml of ethanol and stirred for 1 h to obtain a uniform transparent suspension. Second, 12.68 g of oxalic acid was dissolved in 100 ml of water. After completely dissolving the oxalic acid, the tetrabutyl titanate solution was added and the mixture was continuously and vigorously stirred. Once the initial white precipitate re-dissolved, a clear solution was obtained and referred to as solution A. Simultaneously, solution B was prepared by dissolving 3.92 g of calcium chloride in 200 ml of ethanol/water ($V/V = 9/1$). Solution A was then added dropwise to solution B and vigorously stirred at 25 °C. An opalescent precipitate formed instantly and the mixture was continuously stirred for 6 h before it was aged overnight at a constant temperature of 25 °C. The precipitate was centrifuged and washed with deionized water and ethanol, then it was dehydrated in a vacuum at 60 °C for 12 h and at 110 °C for another 4 h.

Preparation of the ER fluids

All of the silicone oils were dried at 120 °C for 2 h before the experiments to avoid any influence from moisture. The density and dielectric constant for the silicone oil at room temperature were 0.940 g cm^{-3} and 2.5, respectively. The density of the HCTO particle was 2.45 g cm^{-3}. An ER suspension was prepared by dispersing the particles in silicone oil via grinding. In this work, the ER fluid concentration was calculated based on the volume fraction of the ER particles.

Characterization

Powder X-ray diffraction patterns were collected by a Bruker D8 Advance/Discover diffractometer (Bruker, Karlsruhe, Germany) with Cu-Kα radiation. All of the measurements were obtained using a 40 kV generator voltage and

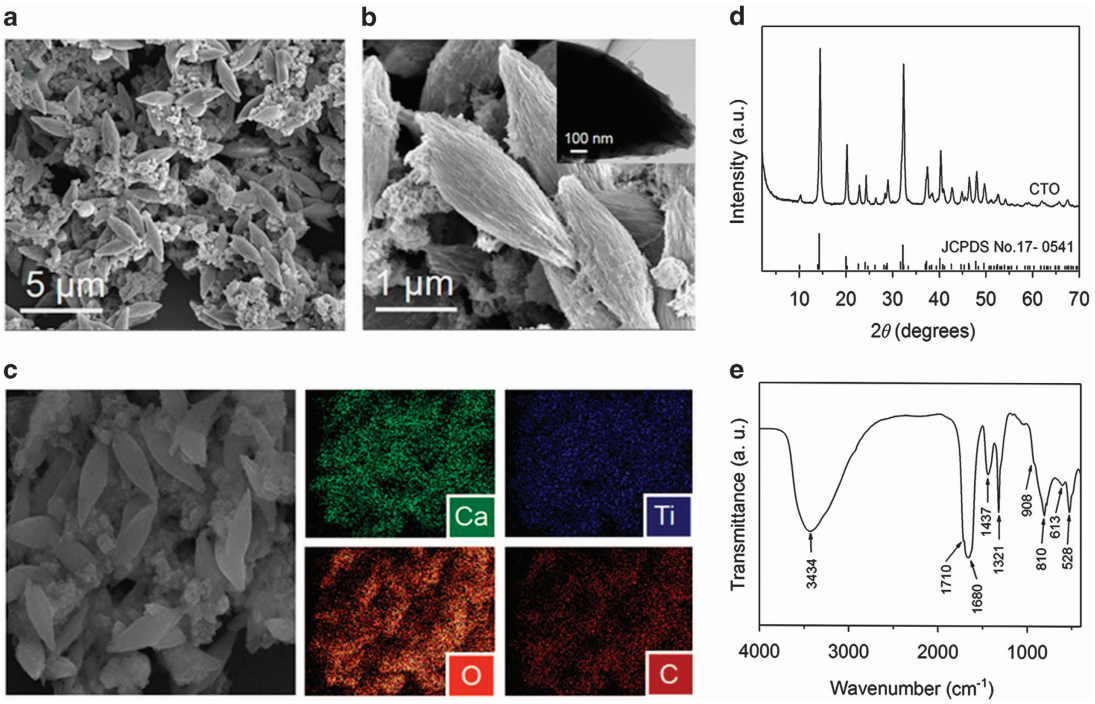

Figure 1 (**a**, **b**) SEM images, (inset in **b**) transmission-electron microscopy image, (**c**) energy dispersive spectroscopy elemental mapping for calcium, titanium, oxygen and carbon elements, (**d**) X-ray diffraction pattern, (**e**) and Fourier transform infrared (FTIR) spectra of the HCTO particles.

40 mA current. The sample morphologies were examined using a Hitachi S4800 field-emission scanning electron microscope (SEM, Hitachi, Tokyo, Japan) and an FEI Tecnai G2 F20 transmission electron microscopy (FEI, Hillsboro, OR, USA). The Fourier transform infrared spectra were recorded using a Nicolet 6700 spectrometer (Thermo Scientific, Waltham, MA, USA).

The rheological properties were measured using a circular rheometer (Haake RS6000, Thermo Scientific) with a circular-plate system (15 mm in diameter with a 1.0 mm gap width). A stress–strain measurement at a low shear rate provided the yield stress and the stress where the viscosity decreased abruptly was defined as the static yield stress. The flow curves for the shear stress–shear rates were measured using the controlled shear rate mode with a rotary cup accessory for the shear rate range from 0.1 to 100 s^{-1}. The gap between the outer cup and the inner bob was 1.0 mm. Each shear rate was maintained for 3 s; thus, it reached equilibrium before data were collected. Experimental data were collected using the Rheowin software package. All of the measurements were performed at room temperature.

RESULTS AND DISCUSSION

HCTO particles were synthesized via the simple co-precipitation of tetrabutyl titanate, calcium chloride and oxalic acid. The SEM and transmission electron microscopy images (Figure 1a and b) show that the HCTO composite consists mainly of micrometer-sized spindly particles and a few irregular nanoparticles. It can be observed from the magnified SEM image (Figure 1b) that the spindly particles are composed of smaller fibrous particles. The average particle length is ~4 μm and the aspect ratio is ~3.3. The elemental distribution (Figure 1c and Supplementary Figure S1) of the HCTO composite was acquired by energy dispersive spectroscopy. The Ca, Ti, O and C elemental mapping images visually identify that these elementals are uniformly distributed within the spindly particles and the tiny irregularly nanoparticles. The anisotropic properties of the spindly particles can enhance the yield stress and ensure their structural stability. In addition, the local electric field is greatly enhanced at the tips of the elliptical particles and the gap regions in the adjacent particles,[15] which amplifies the interacting forces between the polar molecules near the tip apex and should result in an improved ER efficiency. Moreover, the spindly particles in this study were larger than most previously reported CTO particles, which would reduce the field-off viscosity.

The corresponding X-ray diffraction patterns of the HCTO composite are shown in Figure 1d and the calculated values of *d* match well with the reported X-ray data for calcium oxalate dehydrate (JCPDS Number 17-0541). The unidentified lines in the X-ray diffraction patterns can be attributed to hydroxyl titanium oxalate (HTO, $TiOC_2O_4$ $(H_2O)_2$) and $TiO(OH)_2$, as it is difficult to obtain crystalline precipitates of HTO.[32] The Fourier transform infrared spectrum (Figure 1e) was also measured to verify the formation and structure of the HCTO particle. The broad band at ~3434 cm^{-1} is assigned to the –OH stretching vibration. The C = O stretching bands specific to oxalate occur at 1710 and 1680 cm^{-1}. The absorption bands at 1437 and 1321 cm^{-1} are due to the metal–carboxylate

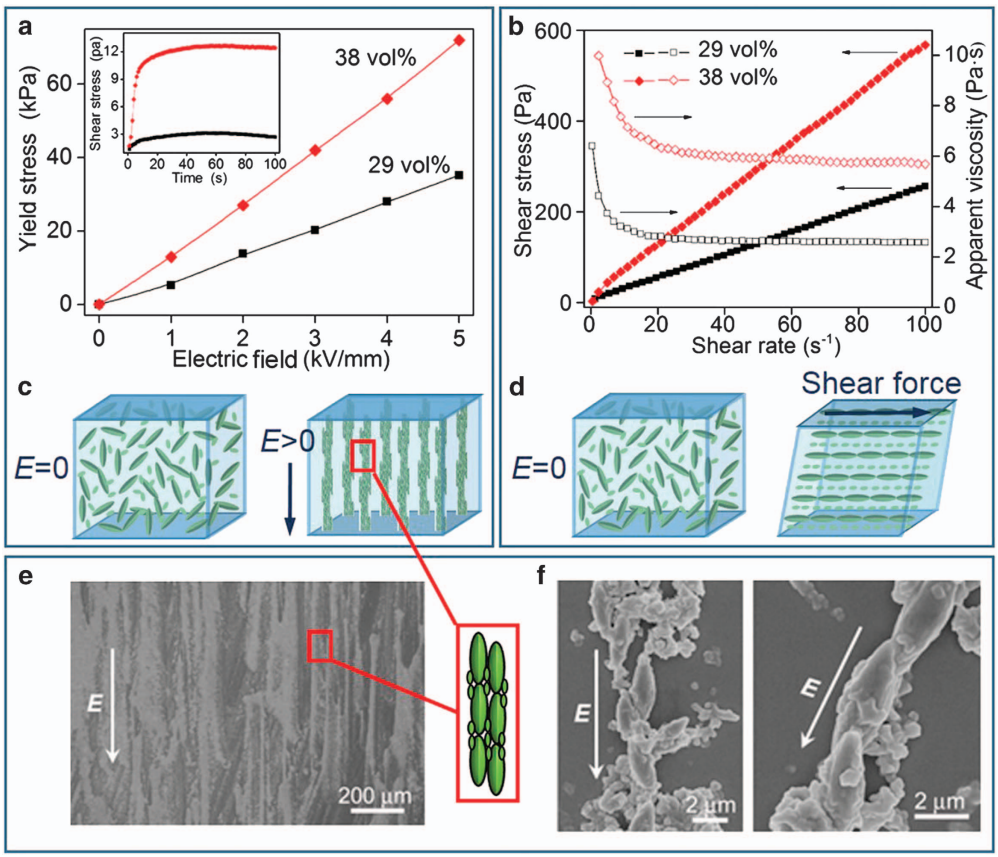

Figure 2 Electrorheological properties for HCTO electrorheological fluids with different concentrations: (**a**) yield stress under different electric fields, inset: the shear stress as a function of time without the applied electric field; (**b**) flow curves as a function of the shear rate without the applied electric field; schematic of the electrorheological structure without/with the applied electric field (**c**) and without/with shear stress (**d**); SEM image of the ER structures of the HCTO suspension between the electrodes under the applied electric field (**e**, **f**).

(M–COO−) symmetric stretching modes. The absorption peak at 810 cm^{-1} is assigned to the C–C vibration band. The band at 528 cm^{-1} is attributable to O–C–O in-plane bending. The shoulder peak at 908 cm^{-1} is consistent with a Ti=O double bond, which should be attributable to the HTO particle and indicates that Ti exists as amorphous HTO in the particles. Inductively coupled plasma (ICP) tests show that the Ca and Ti element contents are 11.49 and 10.56%, which further confirms the existence of HTO. HTO has a key role in ER activity. The wettability between the ER particles and silicone oil, as well as the interactions between different particles, can be improved as a result of the existence of HTO.[33] We systematically compared the wetting performance of the ER particles and silicon oil, and the results show that good wettability can enhance the yield stress and reduce the field-off viscosity effectively.[34] Moreover, the aligned dipolar filaments formed from the hydroxyl titanium oxalate polar groups bridge the two nanoscale confinement boundaries and can penetrate the silicon oil film so that the ER particles and silicon oil interact with each other in the nano-contract region between the two polarizable particles.

The ER behavior of the HCTO ER fluids was evaluated in the presence and absence of the electric field. As shown in Figure 2a, the HCTO ER fluids exhibit distinctly high capacities with yield stresses as high as 35 and 75 kPa when the volume fractions are 29 and 38 vol%, respectively. The yield stress displays near-linear dependence on the electric field strength. In principle, the linear dependence between the applied electric field and the magnitude of the yield stress directly reflects the surface saturation polarization.[7] The magnitude of the yield stress is comparable to that observed in other modified rod-like or core-shell structured CTO ER fluids. However, the field-off viscosities (Figure 2b) are 5.8 and 2.7 Pa s^{-1} at 100 s^{-1}, which are significantly lower than those for rod-like CTO suspensions at the same concentration. ER efficiency is defined as $e=\tau_E/\tau_0$, where τ_E and τ_0 are respectively the yield stresses with and without the applied electric field. According to the experimental values in Figure 2a, the ER efficiency e of the 29 and 38 vol% ER fluids are 12 000 and 6000, respectively. In other words, their yield stresses increase by 12 000 and 6000 times after the external electric field is applied. Compared with those of previously reported ER fluids, the ER efficiency of the HCTO suspension increases by one to two orders of magnitude (Figure 3). This comparison demonstrates that this material provides an excellent platform for the application of GERs. Increasing the particle concentration further would increase the yield stress and the maximum yield stress could be as high as 140 and 255 kPa when the volume fractions are 43 and 49 vol%, respectively (Supplementary Figure S2, the shear stress versus strain curve is also shown in Supplementary Figure S3).

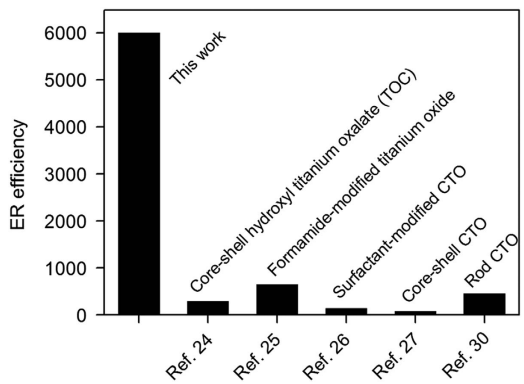

Figure 3 A summary of ER efficiency for this material and other previously reported ER materials.

A schematic illustration of the phenomenon is presented in Figure 2c and d. When no electric field is applied, the spindly microparticles and the tiny nanoparticles are distributed homogeneously in the insulating liquid, while the spindly particles are randomly oriented. On applying an electric field, the polarized particles in the ER fluids aggregate and form chains along the direction of the electric field. The long axis of the spindly particles is parallel to the electric field direction, because the field-induced rotational torque exceeds the thermal forces. These anisotropic particles can engender larger induced dipole moments than the isotropic particles, because their long axis is oriented in the direction of the electric field.[35–38] Moreover, the head-to-head alignment of the spindly particles enhances the local electric field in the junction area, which leads to a considerable and additional rise in the induced dipole moments and interparticle interactions.[16] Simultaneously, the tiny nanoparticles accumulate at the spindly microparticle junctions to form more intense geometrical structures in a manner analogous to that used in concrete construction. This unique structure that increases the friction and mechanical cohesion is greatly beneficial to the chain strength. On the other hand, the induced dipole moment and the field-induced rotational torque of the particles vanish immediately when the external electric field is removed. According to the calculation, the response time is 36 ms (Supplementary Figure S4). The spindly particles can rotate rapidly and maintain their long axis in a parallel direction with the shear flow direction, which results in a sharp decrease in the viscosity of the suspension. As a consequence, the ER efficiency of the HCTO suspension is enhanced by these combined effects. SEM images (Figure 2e and f) confirm the mechanism proposed above.

To further verify the synergistic ER effect of the HCTO material, the spindly and tiny particles were separated through centrifugation. Figure 4a and d show SEM images of the spindly and tiny particles, respectively. The X-ray diffraction and Fourier transform infrared results indicate that the components of the spindly and tiny particles are similar (Supplementary Figures S5 and S6). However, the yield stress (Figure 4b and e) of these single-component ER fluids under an applied electric field clearly decreases compared with that of the composite material. Although the content of the tiny particles is low in the HCTO composite, the tiny particles can enhance the ER activity effectively by gathering at the contact area of the large particles. This further confirms the synergistic effect between the spindly and tiny particles. Furthermore, the field-off stress (Figure 4c and f) and viscosities (Supplementary Figure S7) of the tiny particles are much higher than those of the spindly particles, owing to their small particle size, which results in low ER efficiency.

Dynamic rheological properties were also evaluated to gain a more comprehensive understanding of the HCTO ER fluids (Figure 5a and b). The maximum shear stress is ~ 70 kPa, which is equivalent to the yield stress at the same concentration. It is generally acknowledged that the dynamic rheological behavior is mainly dominated by the shear-field-induced hydrodynamic force and the electric-field-induced electrostatic interaction, wherein the hydrodynamic interactions tend to destroy ER structures and promote flow, whereas the electric-field-induced interactions cause the reorganization of ER structures and hinder flow. It is observed that shear stress could be maintained at a stable level for the entire range of the shear rate under low electric fields and low concentrations (Figure 5a). However, as the electric field increases, especially for the higher concentration suspensions, the shear stress tends to decrease after reaching a maximum (Figure 5b).

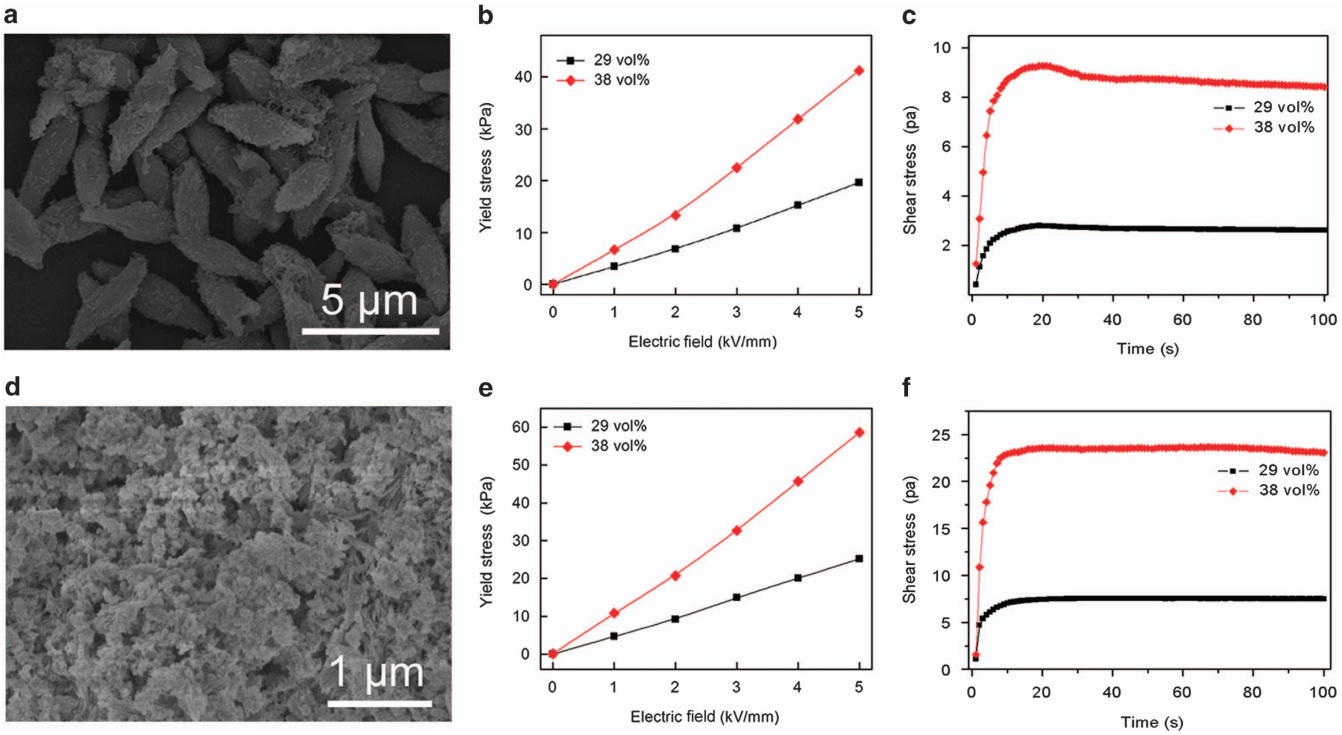

Figure 4 Morphology and rheological behaviors of the spindly and tiny particles after separation: (**a**) SEM images, (**b**) yield stress as a function of electric field and (**c**) field-off shear stress as a function of time under the controlled condition for the spindly particles; (**d**) SEM images; (**e**) yield stress as a function of electric field; and (**f**) field-off shear stress as a function of time under the controlled condition for the tiny particles.

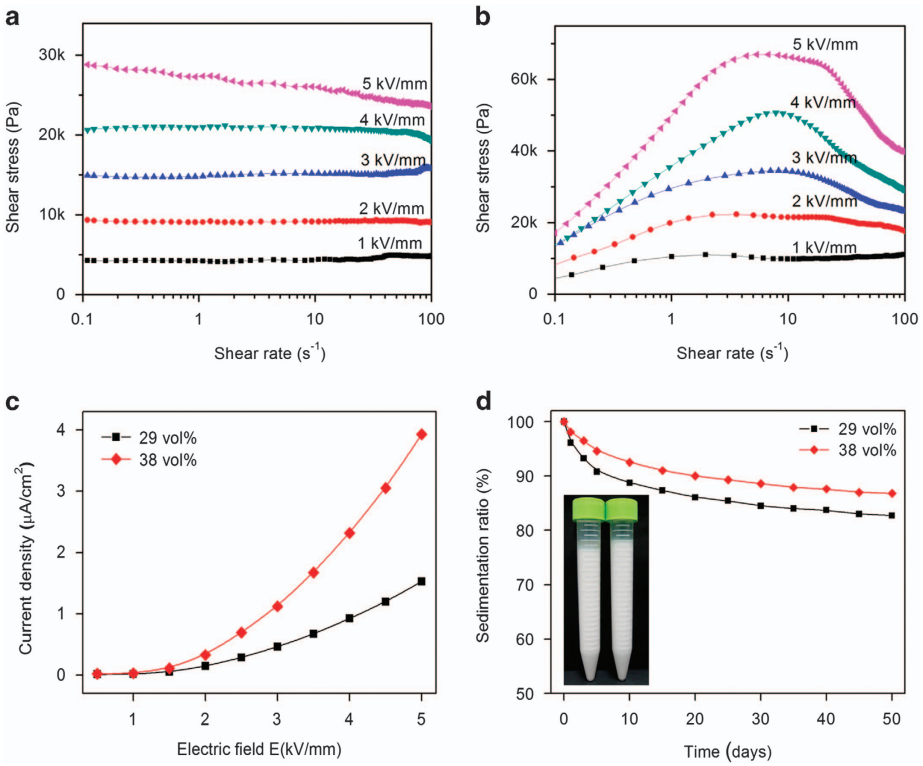

Figure 5 (**a**,**b**) Shear stress (**a**: 29 vol% and **b**: 38 vol%) as a function of shear rate under various electric fields for the HCTO ER fluids; (**c**) current density as a function of the electric field for the HCTO ER fluids; (**d**) time dependence of the sedimentation ratio for the HCTO ER fluids.

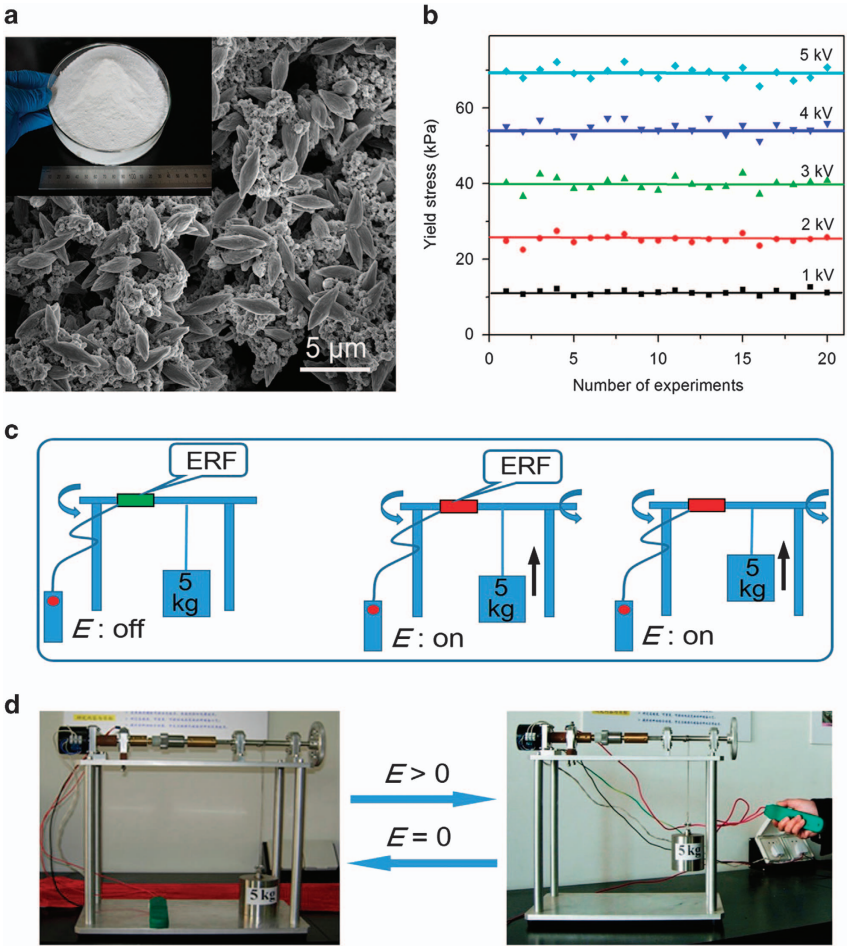

Figure 6 (**a**) SEM images of HCTO particles prepared at a large scale; inset: photo of 200 g of HCTO particles synthesized in a 10 l vessel; (**b**) repeatability results: yield stress under different electric fields for the experiments repeated 20 times; (**c**, **d**) schematic and photograph of the smart transmission shaft demonstration equipment.

In fact, this is a common phenomenon in the parallel-plate measurement apparatus and it was discovered that the suspensions were easily expelled from the central region of the testing apparatus.[19] According to Wen's theory,[28] particles tend to aggregate into fibrous or column-like structures when an electric field is applied. The column structure has a higher density than the fluid and the rotating motion leads to a net centrifugal force that acts outward on the solid structures formed from the particles. The aggregates with a higher density would then migrate to the outer edges of the plate, which results in a net decrease in the measured shear stress. This problem can be effectively prevented by adding a sealed circular annulus outside the parallel plates to confine the ER suspensions. Such a boundary-confined geometry, which is typical for the application of field-activated fluids, was used in previous experiments on GER systems.[19,39]

The leakage current density and the gravitational settling property are important criteria to evaluate whether the ER materials can be employed for a wide range of applications. As shown in Figure 5c, the maximum leakage current density is below 5 μA cm^{-2}. The result indicates that the HCTO material enables high operational safety and lower energy consumption. In general, the gravitational settling property depends on the density mismatch between the ER particles and the silicon oil, as well as the wettability of the particles. The ER activity decreases dramatically along with an increasing phase separation of the ER suspensions. A graduated tube was used to record the sedimentation ratio, which is defined by the height percentage of the solid-rich phase relative to the total height of the suspension. Figure 5d shows that the sedimentation ratios are 83.7% and 87.5% after 50 days. Compared with the sedimentation ratio of ER fluid with tiny particles, the disparity in the sedimentation ratio between the two types of ER fluids is only 1.9% (Supplementary Figure S8). The superiority of the tiny particles is not obvious. There may be two reasons for this phenomenon. First, the densities of the spindly and tiny particles are almost equal, because their compositions are the same. Second, the fine wettability between the CTO particles and the silicone oil contributes effectively to the anti-sedimentation properties. More importantly, no obvious agglomerates were found at the bottom of the graduated tube and slight shaking or grinding can re-disperse the particles and recreate a homogeneous suspension; this should be attributed to the unique morphology of the spindly particles. However, a phase separation was found for the tiny particles (the inset in Supplementary Figure S8) and this phenomenon may be caused by the agglomeration of the nanoscale tiny particles, which do not readily re-disperse.

The approach can be easily scaled up. A 200 g per batch scale-up was successfully achieved in our lab using a 10 l reactor. Figure 6a shows the SEM image of the HCTO sample obtained in the large-scale

process and the particles have similar morphologies to those obtained using the beaker, which implies that the growth of HCTO particles is highly reproducible. More importantly, large-scale experiments were repeated 20 times to verify the potential controllable nature of the preparation process. The ER test (Figure 6b) results show that the yield stress is consistent and stable with a maximum variation of $<6\%$. The HCTO ER fluid showed excellent comprehensive properties. Three pieces of demonstration equipment were designed to verify its performance in practical applications and its aging/durability performance. The first one is a 'smart transmission shaft,' which is the schematic diagram shown in Figure 6c. The motor and the transmission rod are connected by a coaxial cylindrical conductor, which is filled with the HCTO ER fluid, and a soft rope is wound around the shaft with a 5 kg weight connected at the end of the rope. As shown in Figure 6d, in the initial state (Figure 6d left) the motor rotates at a constant speed but the transmission rod does not rotate, because the ER fluid in the coaxial cylindrical conductor is in liquid state. After the power is switched on (Figure 6d right), the motor can drive the transmission rod and the weight is lifted up gradually. In addition, a smart 'fitness bike' and shaking control equipment (Supplementary Figure S9) equipped with ER dampers were designed. For the fitness bike, a continuous variable stress adjustment can be realized by varying the electric field strength. Therefore, an individual can adjust the strength of the bike by controlling the electric field according to the exercise condition desired. The shaking control equipment can be used as a shock absorber in vehicles, as the stress or viscosity of the ER fluids can be adjusted according to the road condition.

CONCLUSIONS

In summary, we successfully prepared a novel micro/nanoparticle HCTO ER material composed of micrometer-sized spindly particles and nanometer-sized irregular particles. The corresponding ER fluids showed enhanced ER activity due to the unique anisotropic morphology of the spindly particle and the synergistic effect between the two types of particles. Under the applied electric field, the nanometer-sized particles gather at the contact area between two neighboring spindly particles and this unique structure effectively enhances the yield stress. The orientation of the spindly particles under the applied electric field was also observed. Under no electric field, the field-off viscosity is reduced due to the large size of the spindly particles, which results in an ultrahigh ER efficiency. In addition, this facile synthesis route may be considered a green chemistry method and it can be scaled up for the industrial production of giant ER materials.

CONFLICT OF INTEREST

The authors declare no conflict of interest.

ACKNOWLEDGEMENTS

This research was supported by the National Natural Science Foundation of China (grants 21573267, 11574331 and 11374311), the Zhejiang Provincial National Science Foundation (LY14B070012), the Youth Innovation Promotion Association CAS (2013196), the Major Project Technology Foundation of Ningbo City (2014S10005) and the program for the Ningbo Municipal Science and Technology Innovative Research Team (2015B11002).

1 Sheng, P. & Wen, W. Electrorheological fluids: mechanisms, dynamics, and microfluidics applications. *Annu. Rev. Fluid Mech.* **44**, 143–174 (2012).
2 Hao, T. Electrorheological fluids. *Adv. Mater.* **13**, 1847–1857 (2001).
3 Yin, J., Zhao, X., Xiang, L., Xia, X. & Zhang, X. Enhanced electrorheology of suspensions containing sea-urchin-like hierarchical Cr-doped titania particles. *Soft Matter* **5**, 4687–4697 (2009).
4 Choi, H. J. & Jhon, M. S. Electrorheology of polymers and nanocomposites. *Soft Matter* **5**, 1562–1567 (2009).
5 Lee, S., Lee, J., Hwang, S. H., Yun, J. & Jang, J. Enhanced electroresponsive performance of double-shell SiO2/TiO2 hollow nanoparticles. *ACS Nano* **9**, 4939–4949 (2015).
6 McIntyre, C., Yang, H. & Green, P. F. Electrorheology of suspensions containing interfacially active constituents. *ACS Appl. Mater. Interfaces* **5**, 8925–8931 (2013).
7 Shen, R., Wang, X., Lu, Y., Wen, W., Sun, G. & Lu, K. The methods for measuring shear stress of polar molecule dominated electrorheological fluids. *J. Appl. Phys.* **102**, 024106 (2007).
8 Tan, P., Huang, J., Liu, D., Tian, W. & Zhou, L. Colloidal electrostatic interactions between TiO_2 particles modified by thin salt solution layers. *Soft Matter* **6**, 4800–4806 (2010).
9 Liu, Y. D. & Choi, H. J. Electrorheological fluids: smart soft matter and characteristics. *Soft Matter* **8**, 11961–11978 (2012).
10 Shin, K.-Y., Lee, S., Hong, S. & Jang, J. Graphene size control via a mechanochemical method and electroresponsive properties. *ACS Appl. Mater. Interfaces* **6**, 5531–5537 (2014).
11 Jiang, J., Tian, Y. & Meng, Y. Structure parameter of electrorheological fluids in shear flow. *Langmuir* **27**, 5814–5823 (2011).
12 Sedlačík, M., Mrlík, M., Pavlínek, V., Sáha, P. & Quadrat, O. Electrorheological properties of suspensions of hollow globular titanium oxide/polypyrrole particles. *Colloid Polym. Sci.* **290**, 41–48 (2012).
13 Zhang, W. L., Liu, Y. D. & Choi, H. J. Graphene oxide coated core–shell structured polystyrene microspheres and their electrorheological characteristics under applied electric field. *J. Mater. Chem.* **21**, 6916–6921 (2011).
14 McIntyre, E. C., Oh, H. J. & Green, P. F. Electrorheological phenomena in polyhedral silsesquioxane cage structure/PDMS systems. *ACS Appl. Mater. Interfaces* **2**, 965–968 (2010).
15 Huang, X., Wen, W., Yang, S. & Sheng, P. Mechanisms of the giant electrorheological effect. *Solid State Commun.* **139**, 581–588 (2006).
16 Tan, P., Tian, W., Wu, X., Huang, J., Zhou, L. & Huang, J. Saturated orientational polarization of polar molecules in giant electrorheological fluids. *J. Phys. Chem. C* **113**, 9092–9097 (2009).
17 Shen, R., Wang, X., Lu, Y., Wang, D., Sun, G., Cao, Z. & Lu, K. Polar-molecule-dominated electrorheological fluids featuring high yield stresses. *Adv. Mater.* **21**, 4631–4635 (2009).
18 Wen, W., Huang, X., Yang, S., Lu, K. & Sheng, P. The giant electrorheological effect in suspensions of nanoparticles. *Nat. Mater.* **2**, 727–730 (2003).
19 Orellana, C. S., He, J. & Jaeger, H. M. Electrorheological response of dense strontium titanyl oxalate suspensions. *Soft Matter.* **7**, 8023–8029 (2011).
20 Wang, B.-X., Zhao, X.-P., Zhao, Y. & Ding, C.-L. Titanium oxide nanoparticle modified with chromium ion and its giant electrorheological activity. *Compos. Sci. Technol.* **2007**, 3031–3038 (2007).
21 Yin, J. B. & Zhao, X. P. Giant electrorheological activity of high surface area mesoporous cerium-doped TiO2 templated by block copolymer. *Chem. Phys. Lett.* **398**, 393–399 (2004).
22 Xu, L., Tian, W., Wu, X., Cao, J., Zhou, L., Huang, J. & Gu, G. Polar-molecules-driven enhanced colloidal electrostatic interactions and their applications in achieving high active electrorheological materials. *J. Mater. Res.* **23**, 409–417 (2008).
23 Wang, X., Shen, R., Wen, W. & Lu, K. High performance calcium titanate nanoparticle ER fluids. *Int. J. Mod. Phys. B* **19**, 1110 (2005).
24 Wu, J., Xu, G., Cheng, Y., Liu, F., Guo, J. & Cui, P. The influence of high dielectric constant core on the activity of core–shell structure electrorheological fluid. *J. Colloid Interface Sci.* **378**, 36–43 (2012).
25 Wu, J., Jin, T., Liu, F., Guo, J., Cui, P., Cheng, Y. & Xu, G. Preparation of rod-like calcium titanyl oxalate with enhanced electrorheological activity and their morphological effect. *J. Mater. Chem. C* **2**, 5629–5635 (2014).
26 Wu, J., Jin, T., Liu, F., Guo, J., Cheng, Y. & Xu, G. Formamide-modified titanium oxide nanoparticles with high electrorheological activity. *RSC Adv.* **4**, 29622–29628 (2014).
27 Cheng, Y., Liu, X., Guo, J., Liu, F., Li, Z., Xu, G. & Cui, P. Fabrication of uniform core–shell structural calcium and titanium precipitation particles and enhanced electrorheological activities. *Nanotechnology* **20**, 055604 (2009).
28 Wen, W., Huang, X. & Sheng, P. Particle size scaling of the giant electrorheological effect. *Appl. Phys. Lett.* **85**, 299–301 (2004).
29 Hong, J.-Y., Choi, M., Kim, C. & Jang, J. Geometrical study of electrorheological activity with shape-controlled titania-coated silica nanomaterials. *J. Colloid Interface Sci.* **347**, 177–182 (2010).
30 Yin, J. B. & Zhao, X. P. Titanate nano-whisker electrorheological fluid with high suspended stability and ER activity. *Nanotechnology* **17**, 192 (2006).
31 Shin, K., Kim, D., Cho, J. C., Lim, H.-S., Kim, J. W. & Suh, K. D. Monodisperse conducting colloidal dipoles with symmetric dimer structure for enhancing electrorheology properties. *J. Colloid Interface Sci.* **374**, 18–24 (2012).
32 Cheng, Y., Wu, K., Liu, F., Guo, J., Liu, X., Xu, G. & Cui, P. Facile approach to large-scale synthesis of 1D calcium and titanium precipitate (CTP) with high electrorheological activity. *ACS Appl. Mater. Interfaces* **2**, 621–625 (2010).
33 Wu, J., Liu, F., Guo, J., Cui, P., Xu, G. & Cheng, Y. Preparation and electrorheological characteristics of uniform core/shell structural particles with different polar molecules shells. *Colloid Surf. A* **410**, 136–143 (2012).
34 Song, Z., Cheng, Y., Guo, J., Wu, J., Xu, G. & Cui, P. Influence of thermal treatment on CTO wettability. *Colloid Surf. A* **396**, 305–309 (2012).

35 Tian, X., Yin, Y., Wang, B., Song, X., Sun, S., Yu, S., Hao, C. & Chen, K. Anisotropic α-Fe_2O_3@TiO_2 core–shell nanoparticles and their smart electrorheological response. *Eur. J. Inorg. Chem.* **2015**, 430–440 (2015).
36 Yin, J., Shui, Y., Dong, Y. & Zhao, X. Enhanced dielectric polarization and electro-responsive characteristic of graphene oxide-wrapped titania microspheres. *Nanotechnology* **25**, 045702 (2014).
37 Shin, K., Lee, S., Kim, J. J. & Suh, K. D. Discrete dipole moments and enhanced electro-rheological properties of dumbbell-shaped, non-spherical particles. *Macromol. Rapid Commun.* **31**, 1987–1991 (2010).
38 Hwang, J.-K., Shin, K., Lim, H.-S., Cho, J.-C., Kim, J.-W. & Suh, K.-D. The effects of particle conductivity on the electrorheological properties of functionalized MCNT-coated doublet-shaped anisotropic microspheres. *Macromol. Res.* **20**, 391–396 (2012).
39 Lu, Y., Shen, R., Wang, X., Sun, G. & Lu, K. The synthesis and electrorheological effect of a strontium titanyl oxalate suspension. *Smart Mater. Struct.* **18**, 025012 (2009).

Supplementary Information accompanies the paper on the NPG Asia Materials website (http://www.nature.com/am)